

Article

Effect of Alternate Wetting and Drying (AWD) and Other Irrigation Management Strategies on Water Resources in Rice-Producing Areas of Northern Italy

Giulio Luca Cristian Gilardi ^{1,*} , Alice Mayer ¹, Michele Rienzner ¹, Marco Romani ² and Arianna Facchi ¹ 

¹ Department of Agricultural and Environmental Sciences, University of Milan, 20133 Milan, Italy; alice.mayer@unimi.it (A.M.); michele.rienzner@unimi.it (M.R.); arianna.facchi@unimi.it (A.F.)

² Centro Ricerche sul Riso, Ente Nazionale Risi, 27030 Castello D'Agogna, Italy; m.romani@enterisi.it

* Correspondence: giulio.gilardi@unimi.it

Abstract: In rice areas with shallow aquifers, an evaluation of alternative irrigation strategies should include the interactions between irrigation and groundwater recharge and reuse, which influence the overall irrigation efficiency. A modelling system composed of three sub-models within a MATLAB framework (a physically based, semi-distributed agro-hydrological model and two empirical models, the former for the channel network percolation and the latter for the groundwater level) was applied to a 1000 ha rice district in the Padana Plain, Italy. The calibrated framework estimates the daily time series of the water supply needed and of the groundwater level for a given irrigation management, based on the inputs provided (agro-meteorology, crop data, soil data, irrigation practices, groundwater table depth upstream of the study area). Five irrigation management strategies, relevant to the area, were compared: (i) wet seeding and continuous flooding (WFL), (ii) wet seeding and alternate wetting and drying (AWD), (iii) dry seeding and delayed flooding (DFL), (iv) dry seeding and fixed-turn irrigation FTI), (v) early dry seeding and delayed flooding (DFLearly). Due to economic advantages, dry-seeded techniques (DFL, FTI) are replacing the traditional WFL in northern Italy. Simulations show that dry seeding leads to a drastic decrease of the water table in April/May, reducing the overall irrigation efficiency of the area, and that DFL (widely adopted in the area) also causes a spike in rice irrigation needs in June when other crops increase their water demand, exposing the area to water scarcity. All the cited management strategies are assessed in the paper and AWD turned out to couple smaller irrigation needs (from June onwards) compared to continuous flooding techniques with a maintenance of the groundwater recharge, especially in the first part of the irrigation season, thus being a recommendable rice management alternative for the study area.

Keywords: agro-hydrological modelling; water-saving irrigation; irrigation groundwater interaction; irrigation efficiency; irrigation management; rice



Citation: Gilardi, G.L.C.; Mayer, A.; Rienzner, M.; Romani, M.; Facchi, A. Effect of Alternate Wetting and Drying (AWD) and Other Irrigation Management Strategies on Water Resources in Rice-Producing Areas of Northern Italy. *Water* **2023**, *15*, 2150. <https://doi.org/10.3390/w15122150>

Received: 18 April 2023

Revised: 19 May 2023

Accepted: 2 June 2023

Published: 6 June 2023



Copyright: © 2023 by the authors. Licensee MDPI, Basel, Switzerland. This article is an open access article distributed under the terms and conditions of the Creative Commons Attribution (CC BY) license (<https://creativecommons.org/licenses/by/4.0/>).

1. Introduction

With its unique environmental adaptability and socio-economic importance, rice is an essential staple food for human nutrition and plays a crucial role in ensuring global food security [1,2]. Since most of the world's rice production comes from irrigated land [3,4], the sustainability of rice systems is currently threatened by water scarcity; over-exploitation of water resources and future decreases in water availability [5] could further challenge the sustainability of these intensively irrigated systems. Researchers are putting a lot of effort into identifying new irrigation strategies, alternative to the continuous flooding irrigation management (WFL), that could on one hand optimize the irrigation water use and on the other hand preserve traditional gravity rice irrigation systems. The introduction of pressurised irrigation systems would reduce water use for rice cropping but would also lead to a large change in the rice landscape all over the world, while increasing production

costs (technology and energy costs) and environmental impacts (for energy use and, in the case of drip irrigation, for the introduction of huge volumes of plastic materials).

In many areas of the world, especially in Eastern and South-Eastern countries, the Alternate Wetting and Drying (AWD) rice irrigation technique has been applied since the early 2000s [6]. When AWD is adopted, paddy fields are subjected to intermittent flooding cycles, carried out only when the soil water status reaches a critical threshold, which can be expressed as a certain value of the soil water potential/content in the root zone (SWP, SWC) or as a specific water level depth (WLD) of the perched water table below the soil surface. Two types of AWD are generally described in the literature: (i) 'mild' or 'safe', if SWP is maintained between soil saturation and -20 kPa ($WLD \leq 15$ cm), (ii) 'severe', if SWP falls below -20 kPa ($WLD > 15$ cm) [7]. Many authors have studied, at the field level, the effects of AWD on different environmental and agronomical aspects, also taking into account its timing during the crop cycle and the severity of the threshold adopted; in [7] (pp. 175–176) 56 different studies were analysed, including 528 comparisons between AWD and WFL. The results showed that, under a safe AWD, the yield did not significantly decrease and the achieved average reduction in water use (irrigation + rainfall) is 23.4%. Another relevant environmental benefit of AWD is the reduction of global warming potential (GWP), which is primarily being ascribed to the reduction of CH_4 , as a consequence of creating an unsuitable environment (oxidised conditions) for methanogenic soil bacteria [8,9]. Most of the studies in the literature have been conducted in Asia and a real understanding of the effectiveness of this technique in other contexts, different in terms of agronomic practices and pedo-climatic characteristics, is still needed.

Water-saving irrigation strategies are usually assessed at the field level, with the objective to reduce water losses considered 'non-beneficial', such as evaporation, surface runoff, seepage and deep percolation [10]. However, when considering large spatial domains, the evaluation of the effects of a massive change in irrigation strategies should include factors that are difficult to be quantified, such as the interaction of irrigation and the groundwater system [11–13]. The coupling of hydrological, crop and water management models is becoming crucial in addressing the effects of new irrigation practices in agricultural areas, as it allows the study of the different phenomena involved in such complex systems [14,15]. 'Physically-based' models (e.g., HYDRUS-1D and 2D/3D, SWAP) [16–19], developed to simulate water movements in the unsaturated soil on the basis of the Richards equation [20] are generally applied at the field level, while more 'conceptual' models (e.g., APEX, SWAT/SWAT+) [4,21–23], usually based on a bucket approach, are implemented to simulate irrigation planning and management over large areas in a distributed or semi-distributed mode, as they require less data and computational effort. In traditional rice-growing areas, where there is a strong interconnection between irrigation and groundwater dynamics, deep percolation from paddy fields and canal networks recharges the water table, which in turn contributes to water discharges in rivers, irrigation networks and natural springs, thus increasing water availability for agricultural areas further downstream and at the same time reducing irrigation water requirements in fields with shallow groundwater conditions. Given this unique environment, the need for a rigorous method to calculate the water fluxes within the system suggests the application of physically based models to better describe the effect of shallow groundwater conditions on the soil water balance.

The north-western part of the Padana Plain in Italy is the most important rice district in Europe [24]. This area is located on the left bank of the Po River, between the Sesia River and the Ticino River (Figure 1) and has been historically characterised by an abundance of surface water, conveyed through an extensive network of unlined irrigation and drainage canals, and by the presence of one of the largest aquifers in Europe. Soils are generally characterised by a coarser texture (loam/sandy-loam) and by higher vertical percolation rates (7.0 – 23.0 $mm \cdot d^{-1}$) than those found in other rice-growing areas of the world [4]. As WFL traditionally adopted in the study area requires huge volumes of water ($16,000$ – $43,000$ m^3/ha) [25], both the increased frequency of water scarcity periods and the

competition for water use between agricultural and non-agricultural demands have pushed the farmers in the last 15 years to the introduction of water saving techniques, in particular the dry seeding followed by a delayed flooding at the 3–4 leaf (DFL) or by a turn-based irrigation (FTI) in years in which water for a continuous flooding after the dry seeding is not available. Dry seeding is adopted nowadays by more than 60% of the farmers. Despite the fact that DFL has brought many advantages to farmers (i.e., reduced working time and economic savings), it is widely believed that it is causing the lowering of groundwater levels in the first months of the agricultural season (April–May), thus reducing the groundwater contribution to water discharges in rivers and irrigation networks and limiting the mid-season water availability for agricultural areas located downstream. Moreover, there is a perception among farmers and irrigation managers that since the introduction of this technique, competition for irrigation water between rice and other crops (e.g., maize) is increasing in June and partially also in July. This could be due to the fact that with DFL the first flooding has been shifted to the beginning of June instead of being conducted in April–May.

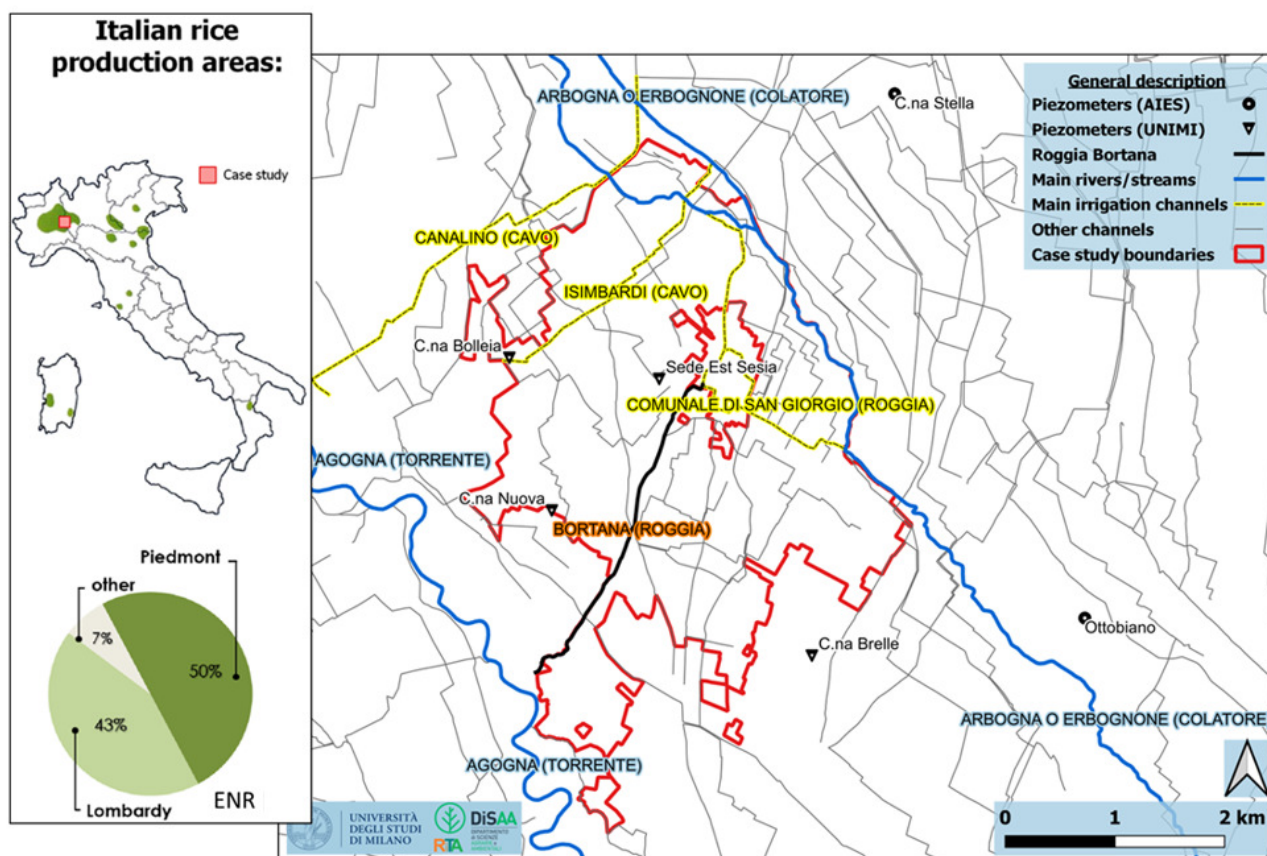


Figure 1. General overview of rice-growing areas in Italy and siting of the pilot irrigation district (San Giorgio di Lomellina, Pavia, Italy).

The year 2022 was characterised by low rainfall and high temperatures in winter, and in spring–summer seasons in Europe, and this highlighted once more the need to rationalise irrigation use in rice areas of northern Italy and better use of the first aquifer. A safe AWD applied after wet seeding could be a solution, ensuring sufficient groundwater recharge in April–May and reducing the rice irrigation need in June–July without yield losses. However, the effects of its introduction on the water resource system should be evaluated in advance.

To achieve this goal, this paper proposes the use of a modelling framework consisting of three sub-models: the first for the agricultural area, based on the well-known physically

based SWAP model [26], the second and the third, empirical, for the groundwater level dynamics and their interaction with the channel network percolation. The modelling framework, calibrated in a previous study [27], was completed by a crop development model and used to explore the effects on the water resource system of realistic scenarios based on the adoption of specific irrigation strategies for rice. The set of the irrigation managements to be tested was chosen in collaboration with the National Rice Authority (Ente Nazionale Risi–ENR) [28] and discussed with the irrigation managers for the rice basin in northern Italy. The chosen set, besides the aforementioned WFL, AWD, DFL and FTI, also includes an early seeding DFL (beginning of April, DFLearly). The DFLearly was conceived to balance the request of farmers that want: (i) to maintain the dry seeding due to economic advantages, (ii) to anticipate the use of water in April–May, where it is usually abundant and no other crops need it, (iii) to recharge the phreatic groundwater at the beginning of the agricultural season. In this study, the modelling framework was applied to a pilot rice district (San Giorgio di Lomellina, Pavia, Italy) for the period 2013–2020.

2. Materials and Methods

2.1. Pilot Irrigation District and Data Availability

The pilot irrigation district, located approximately 45 km south-west of Milan, is in the western part of the municipality of San Giorgio di Lomellina (Pavia, Italy) and covers an area of about 1000 ha (Figure 1).

Hourly time series of the needed agro-meteorological variables were obtained for the period 2013–2020 at a station located approximately 12 km north-west of the district centre (Castello d’Agogna, Pavia, Italy; Agenzia Regionale per la Protezione dell’Ambiente–ARPA Lombardia, Italy) [29]. In the period April–September, the average rainfall, mean air temperature, wind speed at 2 m and daily global radiation were found to be respectively: 326 mm, 21 °C, 2 m/s and 338 W/m².

The irrigation water diverted in the district comes from three canals (Roggia Comunale di San Giorgio–RCSG, Cavo Isimbardi–CiSi and Cavo Canalino–CCan) managed by Associazione Irrigazione Est Sesia–AIES (Figures 1 and 2) [30]. Channel network losses are not quantified; however, they have been estimated to be on average one third of the water discharges during the central part of the agricultural season by AIES. The water table strongly influences percolation losses, which are characterised by higher rates at the beginning of the season (when the water table is deeper) and lower rates at the end of the season.

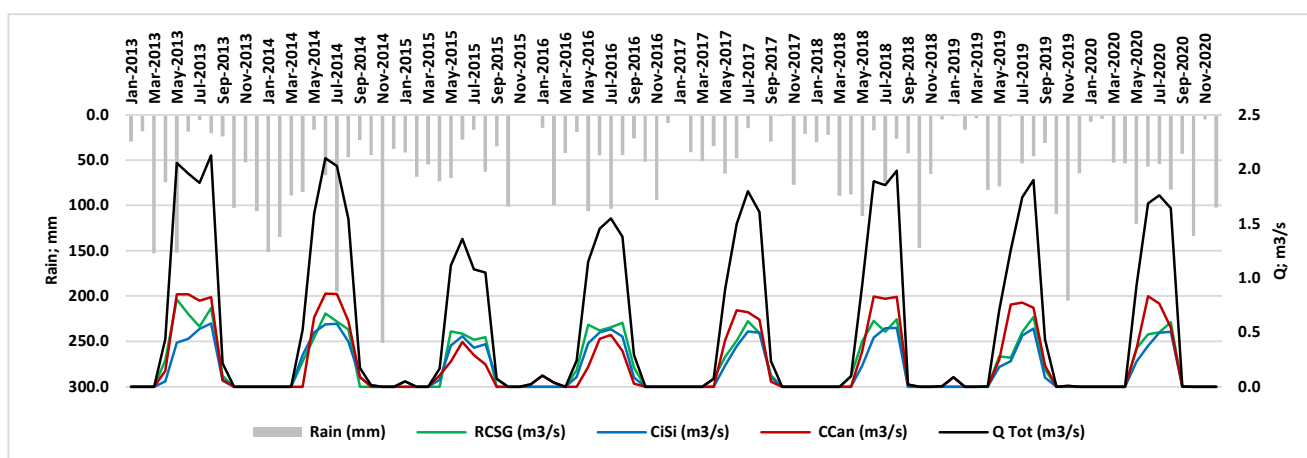
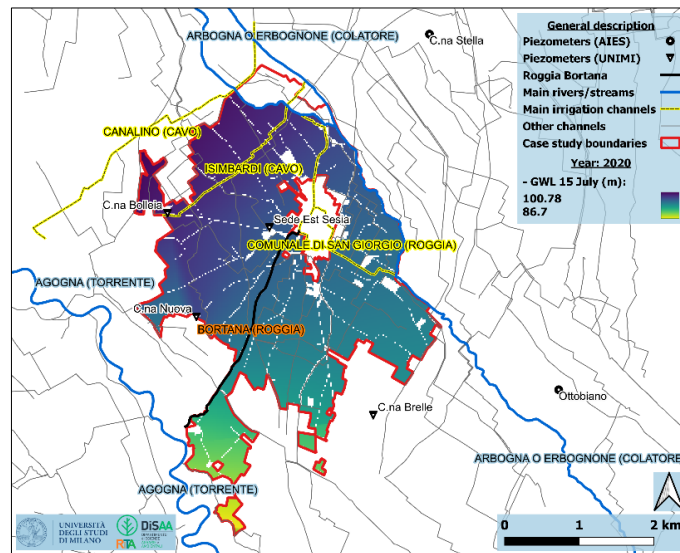
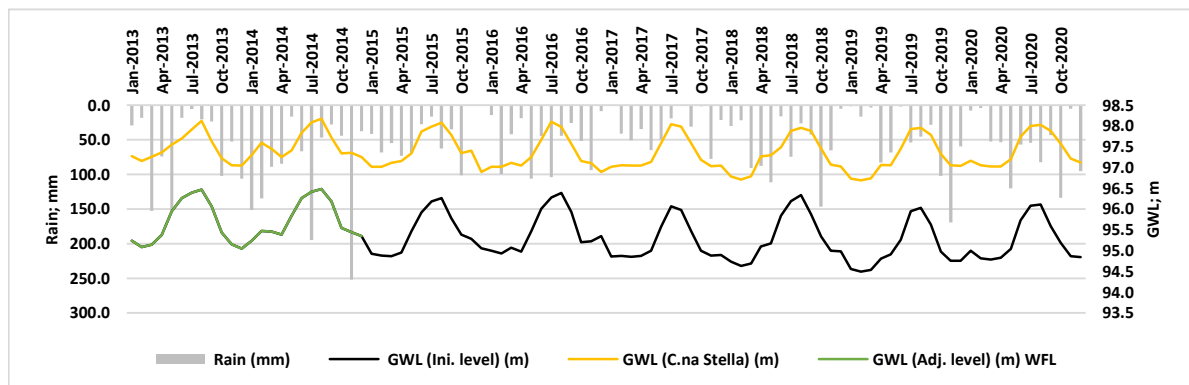


Figure 2. Monthly discharges delivered by AIES in the period 2013–2020. QTot represents the sum of the discharges conveyed by three main channels of the district: ‘Roggia Comunale di San Giorgio’ (RCSG), ‘Cavo Isimbardi’ (CiSi) and ‘Canalino’ (CCan).

As the district is bordered by two rivers (Agogna and Arbogna; Figure 1), the phreatic aquifer is sufficiently hydrogeologically delimited on the east and west sides of the study area, but not in the north and south directions. Groundwater level (GWL) data series representative for the regional aquifer north of the district were obtained from a piezometer located at Cascina Stella ('AIES', Figure 1). Inside the district, GWL has, since 2015, been measured twice a week in four piezometers ('UNIMI', Figure 1) and in another nearby districts (Ottobiano-'AIES', Figure 1). This data (the four piezometers installed by UNIMI and the two from AIES), together with water levels measured in the deep drainage channel Bortana (Figure 1), added as a constant value, were used to interpolate phreatic GWL of the district on July 15th each year during the studied period (2013–2020), as described in [27] (pp. 1838–1839). This date was chosen because the GWL is assumed to be maximum in the district and the obtained map is used by the modelling framework to split the district into two groundwater depth (GWD) sub-areas. For each sub-area, daily spatial interpolations are used to compute two daily GWD series (shallow and deep; see Section 2.2). Figure 3 displays an example of a GWL map built for the day 15 July 2020, together with a comparison of the measured GWL in Cascina Stella (upstream of the pilot district) and in the district (average value) for the period 2013–2020 on a monthly basis.



(a)



(b)

Figure 3. (a) Interpolated reference groundwater level (GWL) of 15 July map (2020); (b) Average monthly groundwater level in San Giorgio and Cascina Stella for the period 2013–2020. Since data for the district were not available for years 13–14, the simulated values obtained from the PGL model (see Section 2.2) for the wet seeding and continuous flooding scenario are shown in green.

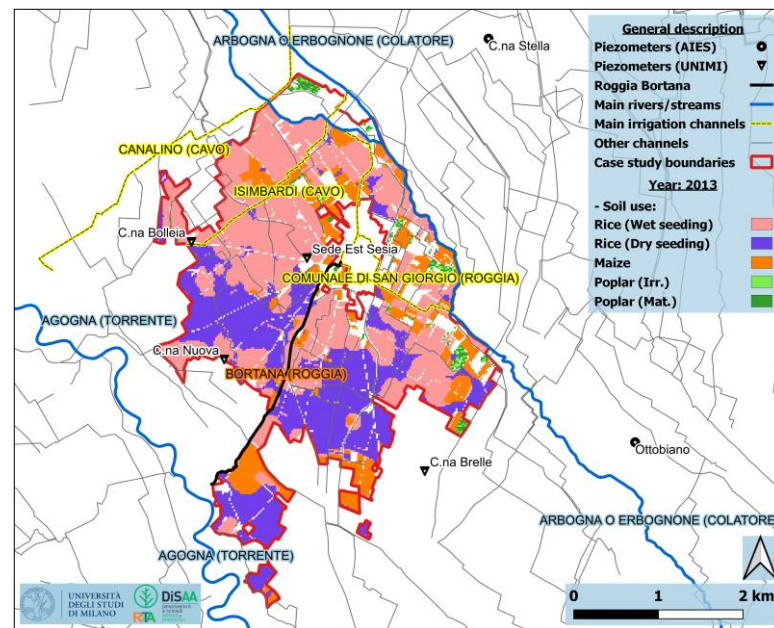
To describe the soils of the district area (Table 1), five units were defined starting from the Soil map of Lombardy (1:50,000; Geoportale Lombardia, Milan, Italy) [31]. Subsequently, the hydraulic properties of each horizon were estimated through PedoTransfer Functions (PTFs). The Bulk Density (BD) was estimated using the PTFs presented in [32], while the parameters of the soil water retention curve ($\theta(h)$) and the saturated hydraulic conductivity (Ks) were estimated using the PTFs presented in [33]. In order to take into account the compaction that characterises paddy field soils, the BD for each soil horizon and the Ks for the less conductive soil layer in the profile were corrected by means of empirical coefficients retrieved by experimental data [27] (pp. 1839–1841).

Table 1. Parameters of the Mualem-Van Genuchten functions [26]. Data are retrieved from [27] (p. 1841). In the last column, values in parentheses indicate saturated hydraulic conductivity (Ks) values modified to account for the compaction of the less conductive soil layer in the profile of paddy field soils.

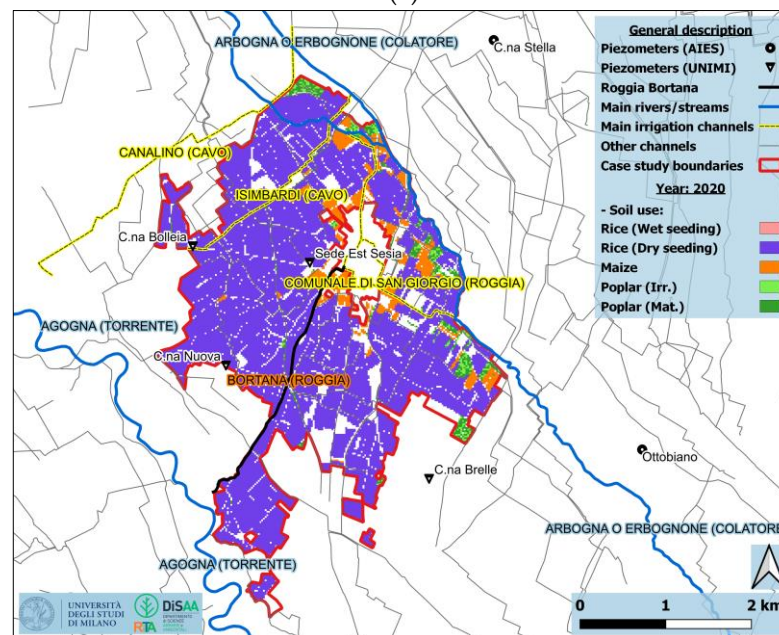
Unit	Depth cm	BD g cm ⁻³	θ_r cm ³ cm ⁻³	θ_s cm ³ cm ⁻³	α cm ⁻¹	n	λ	Ks cm day ⁻¹
407	0–25	1.74	0.0000	0.3348	0.0169	1.2859	0.2859	13.86
	25–50	1.77	0.0000	0.3226	0.0111	1.1940	0.1940	89.20
	50–75	1.77	0.0000	0.3220	0.0154	1.1610	0.1610	88.82(0.97)
	75–105	1.55	0.0000	0.4034	0.0244	1.8436	0.8436	109.61
	105–120	1.58	0.0052	0.3926	0.0688	1.1940	0.1940	114.48
409	0–40	1.65	0.0000	0.3686	0.0467	1.1451	0.1451	56.78
	40–67	1.54	0.0008	0.4071	0.0467	1.3479	0.3479	365.84
	114–150	1.65	0.0496	0.3675	0.0347	1.1352	0.1352	16.33(0.18)
	192–228	1.49	0.0537	0.4263	0.0470	1.6820	0.6820	283.34
410	0–25	1.72	0.0000	0.3400	0.0295	1.1053	0.1053	1.31
	25–40	1.69	0.0043	0.3537	0.0186	1.2098	0.2098	22.52
	40–70	1.63	0.0447	0.3761	0.0261	1.1365	0.1365	14.15(0.15)
	70–100	1.68	0.0584	0.3562	0.0318	1.1319	0.1319	27.01
	100–160	1.62	0.0401	0.3769	0.0877	1.1940	0.1940	225.56
413	0–22	1.65	0.0453	0.3660	0.0697	1.1073	0.1073	2.71
	22–29	1.78	0.0000	0.3194	0.0295	1.1940	0.1940	28.86(0.32)
	29–60	1.68	0.0541	0.3558	0.0336	1.0772	0.0772	132.60
	60–104	1.46	0.0252	0.4397	0.0634	1.6115	0.6115	214.05
	104–117	1.57	0.0000	0.3961	0.0571	1.9240	0.9240	263.97
117–157	1.43	0.2235	0.4510	0.1660	1.1940	0.1940	28.78	
417	0–35	1.72	0.0000	0.3420	0.0301	1.0922	0.0922	1.03
	35–40	1.74	0.0000	0.3346	0.0091	1.2955	0.2955	37.58(0.41)
	40–85	1.77	0.0000	0.3239	0.0162	1.0704	0.0704	136.27
	85–140	1.73	0.0000	0.3389	0.0122	1.2200	0.2200	47.83

The land use map of the area is available on a yearly basis (20 m × 20 m raster maps; Geoportale Lombardia) [31]. The rice-growing area of the district covers approximately 90% of the agricultural surface, while the remaining 10% is cultivated mainly with maize and poplar (Figure 4). The Modified Normalized Difference Water Index (MNDWI) [34], calculated starting from Landsat 7/8 and after 2016 from Sentinel-2 images for the period April–May, when flooding starts in wet-seeded paddies, was calculated every year to identify wet seeded and dry seeded rice areas [27] (pp. 1841–1842). Regarding crops, as poplar is only irrigated in the first four years out of ten (poplar cycle) and covers a very limited area in the district, the poplar area was randomly divided into young (irrigated) and mature (rainfed), following a 40–60% ratio. Maize, also covering a limited area, was considered to follow a fixed development cycle, with emergence on 20th April and harvest on 3rd September. As regards rice, development stages were computed through a crop

module described in Section 2.3. Crop parameters (crop coefficients, rooting depths, Leaf Area Index) for rice, maize and poplar are the same as in [27] (p. 1844).



(a)



(b)

Figure 4. (a) Soil use of the year 2013; (b) Soil use of the year 2020. The transition between wet and dry seeding is particularly evident in the case study area.

2.2. Modelling Framework

The modelling framework consists of three sub-models: (i) one for the agricultural area (SDMAA), based on the well-known SWAP model, (ii) one for the channel network percolation (CP), (iii) one for the GWL dynamics (PGL). The MATLAB code described in [27] (pp. 1844–1849) to integrate the three sub-models and to process the results was further developed in this study. Figure 5 illustrates the flowchart of the model framework showing the interconnections among the three sub-models.

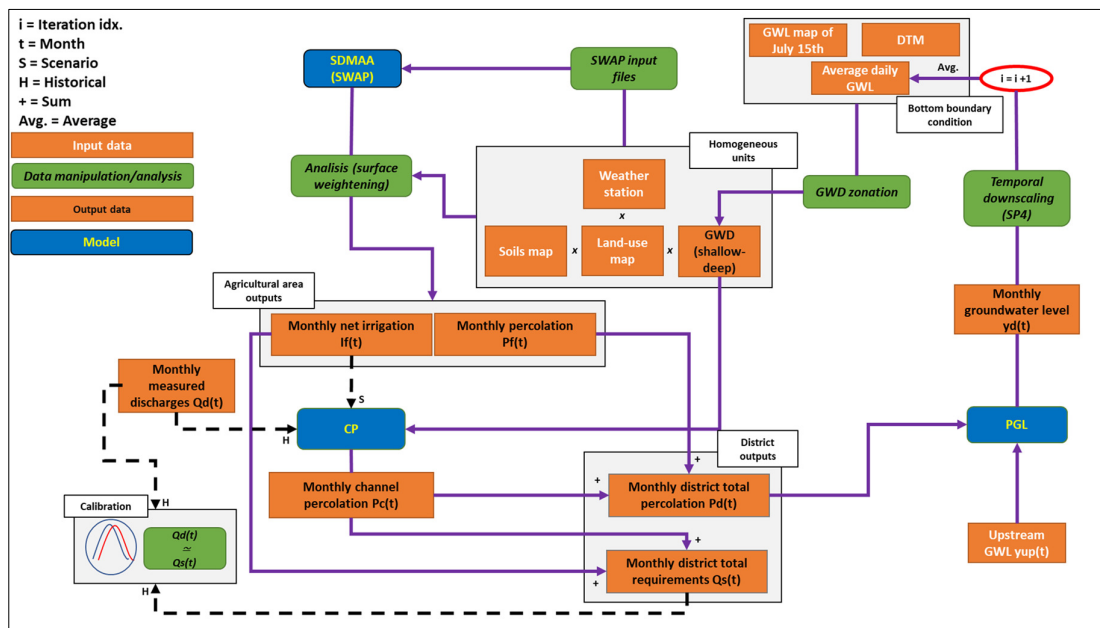


Figure 5. Flowchart of the model framework showing the interconnections among the three sub-models (SDMAA, CP and PGL; see Section 2.2) and the input data required (groundwater level–GWL map of 15 July, Digital Terrain Model–DTM, average daily groundwater level–GWL, weather station, soils map, land-use map and upstream groundwater level–GWL). In the present study only the scenario (S) path was used, since it was not possible to rely on historical (H) measurements of the monthly measured discharges entering the district (Q_d) for the simulated irrigation management alternative. The entire modelling framework, with the exception of the SDMAA core model (SWAP), was developed in MATLAB.

For each year and iteration step, the interpolated GWL map of 15 July, along with the Digital Terrain Model–DTM (20 m × 20 m raster map; Geoportale Lombardia, Italy) [31], is used to create a reference GWD map to split the district into two GWD sub-areas: shallow if greater than −1 m and deep if lesser than −1 m (Figure 6). Then, an interpolation of the GWD for the district is performed for each day of the simulated year and the required series for the SWAP simulations (GWD shallow and deep) are created by averaging the daily values of the GWD maps over the two reference GWD sub-areas. In this step, the actual simulation domain is also defined by overlaying each matrix (20 m × 20 m), showing the spatial distribution of the different information taken into account. SDMAA subdivides the agricultural area of the district into homogeneous simulation units, each one described by a specific set of parameters (SWAP inputs text file), considering crop type and irrigation management, soil type and GWD conditions. The water discharges provided by the three channels (RCSG, CiSi and Can) of the district are distributed homogeneously over the entire agricultural area; due to the limited extension of the district, the same is done for the agro-meteorological data measured in the Castello D’Agogna meteorological station. Once the simulations for each simulation unit are completed, the water fluxes obtained by SWAP are aggregated over a specific time step (e.g., month) to get the monthly net irrigation (I_f , mm) and the monthly percolation (P_f , mm) coming from the agricultural area. Therefore, in order to obtain the district fluxes (m^3), the aggregated results for each unit (mm) are: (i) assigned to the simulation domain based on their position in the district, (ii) weighted (i.e., averaged) over the total cell numbers evaluated in the assigning process, (iii) multiplied by the total surface (total cell numbers evaluated multiplied by the cell size–400 m^2) covered by all the simulated cells within the district domain.

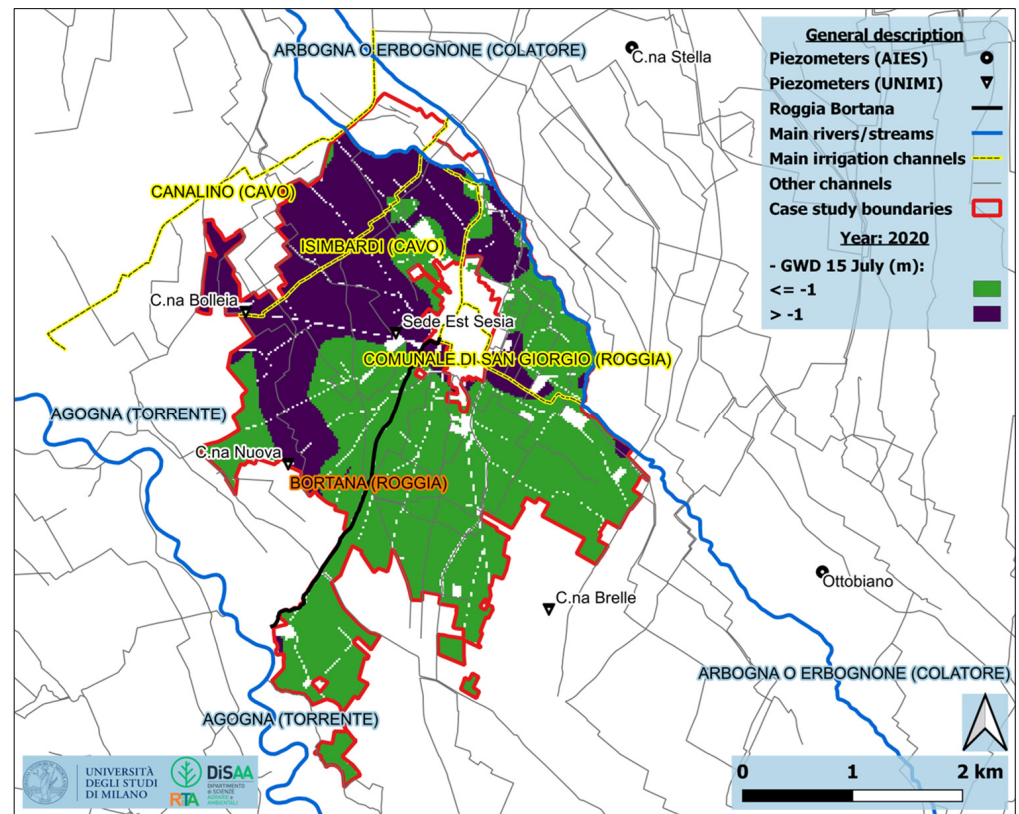


Figure 6. Reference groundwater depth (GWD) map of July 15 used by the framework to subdivide the district into two groundwater depth sub-areas: shallow if greater than -1 m and deep if lesser than -1 m.

Two empirical models complete the modelling framework—the former (PC) is used to estimate the monthly percolation from the channel network (P_c , mm) and the latter (PGL) to simulate the average monthly GWL over the district (y_d , m). In a scenario analysis, in which the monthly measured discharges entering the district (Q_d , mm) cannot be measured, P_c , which is usually highest in the early months of the irrigation season, is estimated as:

$$P_c(t) = \frac{\alpha(t) \times I_f(t)}{1 - \alpha(t)} \tag{1}$$

where $\alpha(-)$ is a loss factor, calculated as follows:

$$\alpha(t) = \begin{cases} 0.2, & t < 4 \text{ or } t > 9 \\ \min(0.4, \max(0, y_d^i - 1.6)), & 4 \geq t \leq 9 \text{ (} t = \text{month, } i = \text{iteration index)} \end{cases} \tag{2}$$

To reproduce the behavior that links the monthly total percolation coming from the district (P_d , mm; $P_f + P_c$) and y_d , in a context in which the district phreatic aquifer is not completely hydrologically isolated, the following theoretical model was chosen:

$$y_d(t)^i = f(P_d(t)^i; y_{up}(t); y_d(t-1)^i); t = \text{month, } i = \text{iteration index} \tag{3}$$

where y_d is the estimated average monthly GWL over the district and y_{up} (m) is the average monthly GWL measured in a piezometer located upstream along the main groundwater flow direction with respect to the study area (C.na Stella). In this way, by following a recursive computation scheme, in which at each iteration step the new GWL (y_d^{i+1}) is averaged with the GWL of the previous iteration step (y_d^i), the modelling system can

simulate scenarios and/or past years for which GWL data are not available. Since the PGL works at a monthly time step, whereas the time step of the GWD series required for the SWAP is daily, the framework also downscales the monthly estimated values to a daily time resolution using an ad-hoc set of fourth-order polynomial curves (SP4) suited for producing daily data series having a monthly average equal to the value of the parent monthly series.

2.3. Model Calibration

The modelling framework was calibrated using historical data for the period 2015–2016 [27] (pp. 1849–1850). For that period, five soil agricultural uses (wet and dry seeded rice, maize, mature and young poplar) were considered; two concerned the rice crop, since the wet seeding and continuous flooding (WFL) and dry seeding and fixed-turn irrigation (FTI) strategies were both used for rice irrigation in the district (WFL with decreasing importance from 2013 onwards).

The calibration of the SDMAA model consisted in a manual tuning of the parameters related to the irrigation management, in particular irrigation amount and application turns, and was conducted together with the calibration of the parameters involved in the PC model. In the calibration process, the objective was to minimise the differences between Q_d and the simulated monthly district total requirements (Q_s , mm; $I_f + P_c$), paying particular attention to the central months of the irrigation season (June, July and August). Specifically, the difference between the measured Q_d and the simulated Q_s in 2015 was used to calibrate the groundwater depth at which channel percolation reaches its maximum (Equation (2)). The Nash-Sutcliffe Model Efficiency (NSME) [35] computed over the whole 2015–2016 period was 0.67, reaching 0.80 when considering just the months characterised by the major channel water losses (April–July).

The calibration of the parameters included in the PGL model was performed automatically, through the MATLAB 'lsqnonlin.m' function, by comparing the available measured GWD and the estimated GWD for the period 2015–2016. The NSME index, averaged over the two GWD (shallow and deep), was 0.89 for the whole two-years period, while it was 0.98 when considering only the irrigation season (15 April–15 September) of the same two years.

2.4. Simulated Scenarios

The simulation scenarios are defined by the irrigation management practice adopted for the rice crops in a whole district. As described in the introduction, the irrigation practices selected for the assessment are: (i) wet seeding and continuous flooding (WFL), (ii) wet seeding and Alternated Wetting and Drying (AWD), (iii) dry seeding and delayed flooding (DFL), (iv) dry seeding and fixed turn irrigation (FTI), (v) early seeding DFL (DFLearly).

Given the nature of the scenario analysis implemented, maize and poplar crop development stages, crop parameters and irrigation management remained the same as described in [27] (pp. 1849–1850) in all of the simulations performed. Maize is border irrigated when a critical threshold of depletion of the Readily Available Water in the root zone (RAW) is reached: (i) in the case of shallow groundwater, irrigation starts when 60% of RAW is consumed and an irrigation depth of 110 mm is applied, (ii) in the case of deep groundwater, irrigation starts when 70% of the RAW is consumed and an irrigation depth of 180 mm is applied. For young poplar (irrigated), two flooding irrigations with a fixed irrigation depth of 150 mm are prescribed, the first at the end of June and the second towards the end of July. For mature poplar (rainfed), no irrigation is simulated, as indicated by AIES.

For the two main types of rice (wet and dry seeded) a crop development model was implemented using a degree days approach analogous to the one used in SWAP from seeding to harvest; moreover, a simple algorithm to determine a likely seeding date for the crop was also implemented. The model allows us to adapt the simulated irrigation management to the differences in crop development occurring each year, associating

eventual changes in the irrigation strategy (e.g., from flooding to turned irrigation) to specific values of the crop Development Stage (DVS). For each year, the seeding date was identified verifying the achievement of a minimum temperature threshold ($T_{seeding}$, °C) in a forward five-days moving window built from a minimum seeding date (D_{min}) up to a maximum seeding date (D_{max}). When D_{max} is reached, even if the air temperature criterion is not satisfied, seeding is forced to occur. The minimum air temperature condition is verified as follows:

$$\frac{\sum_{i=D_{min}}^{D_{min}+4} T_{mean}}{5} \geq T_{seeding} \quad (4)$$

where T_{mean} (°C) is the daily mean air temperature. Three different growing stages were used to describe the development of rice: (i) from seeding to emergence, (ii) from emergence to flowering (DVS from 0 to 1), (iii) from flowering to complete ripening/harvest (DVS from 1 to 2). The thermal contribution of the day (T_{eff} , °C) was computed using the following procedure:

$$T_{eff} = \begin{cases} 0, & T_{mean} < T_{base} \\ T_{mean} - T_{base}, & T_{base} \leq T_{mean} \leq T_{cutoff} \\ T_{cutoff} - T_{base}, & T_{mean} > T_{cutoff} \end{cases} \quad (5)$$

where T_{base} and T_{cutoff} (°C) are the minimum and the maximum temperatures for crop development in a specific growing stage range. Finally, to estimate the DVS value of the crop in a specific day, an integration is performed using the equation:

$$DVS^{i+1} = DVS^i + \frac{T_{eff}}{T_{sum}} \quad (6)$$

where i (–) is the day index, while T_{sum} (°C) is the thermal amount defined to satisfy the achievement of a growing stage. The model was calibrated with the support of the National Rice Authority (Ente Nazionale Risi-ENR) using the year 2020 as the reference and with the aim of obtaining an average crop cycle of around 140 days, with seeding in late April and harvesting around mid-September ($T_{seeding}$, $T_{base} = 10$ °C, $T_{cutoff} = 40$ °C, T_{sum} -DVS: 0–1 = 1051 °C, T_{sum} -DVS: 1–2 = 752 °C). D_{max} was set to be D_{min} plus 30 days for each seeding type. Each scenario inherits its crop development based on the seeding type: (i) wet seeding for WFL and AWD, (ii) dry seeding for DFL, FTI and DFLearly. D_{min} for wet seeding was set to 30th April and for dry seeding to 23rd April. Lastly, in DFLearly, D_{min} was anticipated to 5th April.

With respect to the implementation of the irrigation strategies explored in the scenarios, data were taken from the actual practices adopted by the farmers in northern Italy and, in the case of AWD, from two recent experimentations carried out at CRR-ENR (Centro Ricerche sul Riso; Castello D'Agogna, Pavia, Italy).

In WFL, as an average over the territory, 12 cm of ponded water is maintained on the fields from about five days before seeding until ripening, apart from a few dry periods necessary for plant emergence and other agronomic practices (typically two before and one after the tillering stage, as suggested by ENR).

DFL and FTI are designed based on the currently implemented on-farm practices adopted in northern Italy. In DFL, rice is dry seeded and fields are flooded from the tillering phase up to the ripening phase maintaining about 12 cm of ponding water in the fields. The FTI is managed at the same way as the DFL in the first part of the season (dry seeding), but from the tillering phase onwards, apart from an initial flooding period of about 10 days, rice is irrigated with an eight-day rotation and 120 mm per irrigation event. According to the information provided by AIES, an eight-day rotation is still representative of a good surface water availability for the district.

Concerning AWD, an experimental platform was set up in the agricultural season 2021–2022 at the CRR-ENR to test wet seeding and two different AWD strategies, one safer and one stronger in terms of soil water status critical thresholds of intervention, compared to the traditional WFL. Irrigation water use was monitored by the installation of flow meters and all the other soil water balance components were quantified. In the safe implementation of AWD, the water level depth (WLD) below the field surface, measured in a perforated water tube, could not fall below $-10/15$ cm (corresponding to a SWP at -5 cm of approximately -5 kPa), while in the stronger implementation, the WLD could fall as low as $-20/25$ cm (SWP at -5 cm of approximately -20 kPa). In the field trials, the safe AWD and the strong AWD resulted in saving 25% and 31% of water, respectively, over two years, without showing any drop in production despite a period with scarce water availability for irrigation in 2022, which forced a longer AWD cycle than planned. Moreover, during the agricultural season 2019–2020, the safer AWD was compared with WFL and DFL in a previous experiment carried out at CRR-ENR. At the field scale, water savings of AWD and DFL were found to about 20% and 14% compared to WFL, without penalising rice production [36,37]. Regarding the implementation in the model, AWD is managed as WFL in the early part of the season (wet seeding) and intermittent flooding only starts from the tillering stage, when irrigation is performed to reach 12 mm of standing water only if the soil reaches a critical moisture level of -10 kPa at 5 cm below the soil surface.

No experimental data are available for DFLearly, which is designed in this study to find a compromise between the request of farmers who would like to keep dry seeding due to economic advantages and the need to anticipate the use of water in April–May, recharging the phreatic groundwater at the beginning of the agricultural season. DFLearly maintains the same irrigation scheduling of DFL (dry seeding and flooding from the tillering phase up to the ripening) but implements an earlier seeding date (5th April) than the original DFL (23rd April). Anticipating seeding could lead to an earlier rise in the water table in the first part of the irrigation season, limiting the negative effects of dry seeding.

Hence, in the final configuration used in this study, the model considers 40 simulation units: four crop types cultivated in the area (rice, maize, young and mature poplar), five soil units and two GWD. Each specific rice irrigation alternative (WFL, AWD, DFL, FTI and DFLearly) is applied to all the rice area cropped within the district, while surfaces devoted to maize and poplar remain unchanged. To correct the estimated mean monthly groundwater level over the district (recursive averaging of y_d^{i+1} and y_d^i) based on the simulated monthly total percolation coming from the district (P_d), five iterations for each year are performed ($i = 5$). PC and PGL models use a 30-day time-step, thus the same period is used to aggregate the water fluxes obtained by SWAP in the SDMAA model.

2.5. Performance Indicators

Three indicators (–) were used to support the analysis of results (Water Application Efficiency–WAE, Distribution Efficiency of the irrigation network–DE and Relative Water Supply–RWS) [38,39] calculated both for the whole irrigation season (April–September) and for the most critical month of the irrigation season (June). The equations used to calculate the indicators are:

$$WAE = \frac{ETp_f}{(I_f + R)} \quad (7)$$

$$DE = \frac{I_f}{\frac{Q_s}{g}} \quad (8)$$

$$RWS = \frac{(Q_s + R)}{ETp_f} \quad (9)$$

where ET_{pf} (mm) is the potential evapotranspiration from the agricultural area, I_f (mm) is the net irrigation supplied to the agricultural area, R (mm) is the rainfall, and Q_s (mm; $I_f + P_c$) is the simulated monthly district total requirement.

3. Results and Discussion

3.1. Rice Development Stages

Rice development stages obtained for the period 2013–2020 are shown in Figure 7. Apart from early dry seeding and delayed flooding (DFLearly) in 2013, the minimum seeding date (D_{min}) imposed for each rice seeding type/scenario (dry, wet and DFLearly) and year combination was satisfied; the temperature threshold ($T_{seeding}$) of 10 °C was generally met in D_{min} .

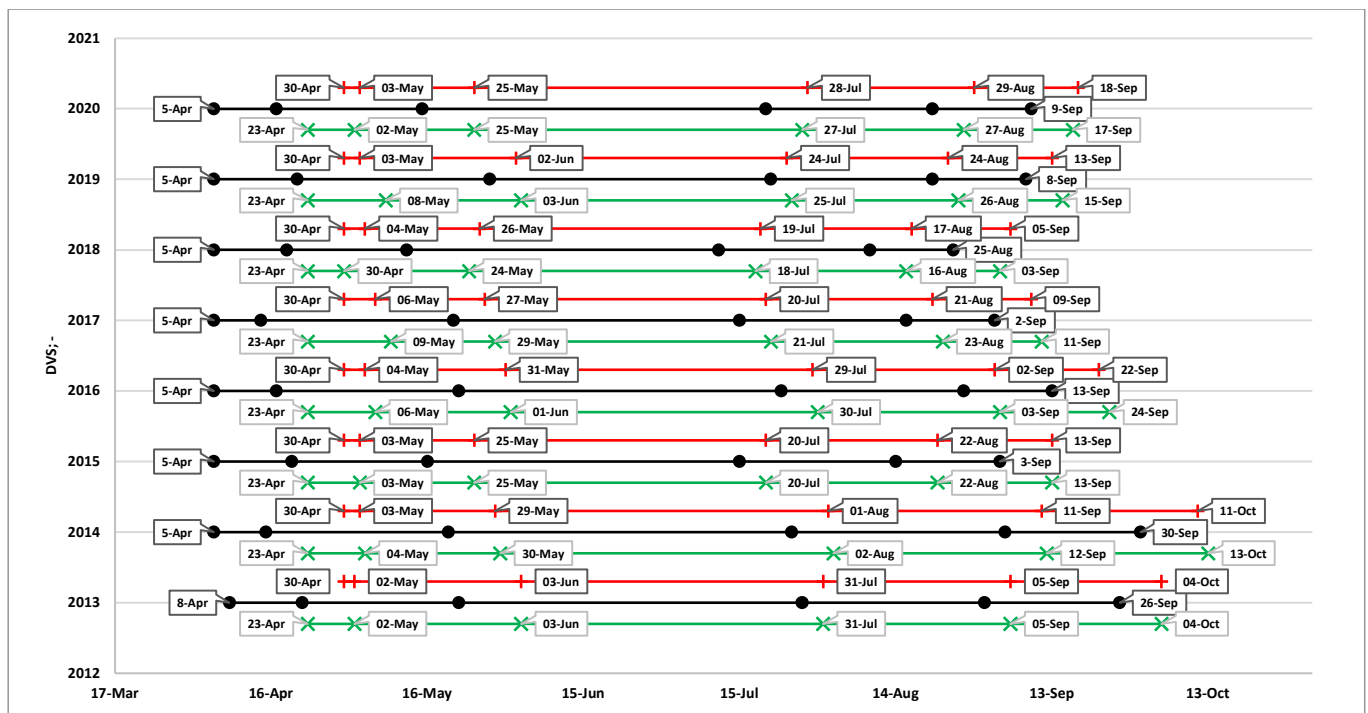


Figure 7. Development stages (DVS) of rice for the years 2013–2020. Lines in black show the development calculated for the early dry seeding and delayed flooding. For each year, the line above the black one reports the development of the scenarios with wet seeding (continuous flooding and alternate wetting and drying, in red), while the line below the black one illustrates the development of the scenarios with dry seeding (delayed flooding and fixed-turn irrigation, in green). The labels indicate (from left to right): (i) seeding, (ii) emergence (DVS = 0), (iii) beginning of tillering (DVS = 0.20), (iv) flowering (DVS = 1), (v), ripening (DVS = 1.65) and (vi) complete ripening/harvesting (DVS = 2). For early seeding, dry seeding and delayed flooding, just the DVS = 0 and DVS = 2 labels are shown.

3.2. Groundwater Depths

The daily simulated groundwater depths (GWD) for all the scenarios are shown in Figure 8. Dry seeding and delayed flooding (DFL) and dry seeding and fixed-turn irrigation (FTI) leads to a drastic decrease in water table levels in the first months of the season, slowing its rise towards its peak (late July–August). In contrast, water table depths in wet seeding and Alternate Wetting and Drying (AWD) overlap with those in wet seeding and continuous flooding (WFL) in the early part of the season and only begin to diverge from the tillering phase (late May–early June). However, from this point onwards, the depths in AWD will never reach the values of WFL, DFL and DFLearly, showing a deeper condition in the middle months of the irrigation season. This is also the case in FTI, which shows similar groundwater dynamics to AWD in the middle months of the

season, although in this scenario the groundwater levels seem to be more influenced by the presence/absence of rain. As expected, early seeding in DFLearly contributes to a rise in groundwater levels at the beginning of the irrigation season to an extent that it is closely linked to rainfall events in the early months of the season compared to the wet seeding scenarios (WFL and AWD). In WFL, the groundwater depths are clearly less influenced by the amount and seasonal patterns of rainfall but depend mainly on the high percolation coming from the agricultural area imposed by the continuous flooding condition. Under good conditions of water availability in rivers and canals, wet seeding is the best option to store water resources in the phreatic aquifer at the beginning of the irrigation season and it is best to make them available for the agricultural area in the following months.

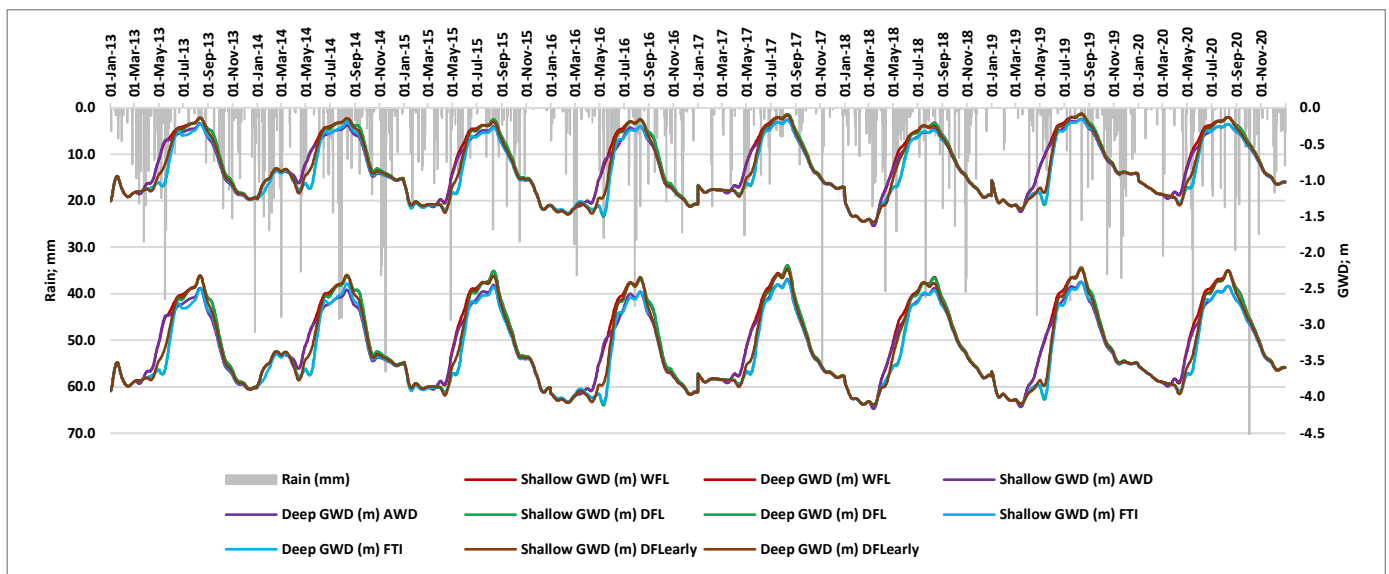


Figure 8. Daily groundwater depths (GWD, shallow and deep) simulated for the years 2013–2020.

3.3. Water Requirements

The average (2013–2020) seasonal (April–September) and critical (June) district total requirements (Q_s : sum of net irrigation from the agricultural area– I_f and the percolation from the channel network– P_c) are reported in Figure 9. The highest seasonal district water use is observed in WFL (19.7 Mm³), followed by AWD and DFLearly (about –16%), DFL (–19%) and FTI (–32%). The lower DFL and FTI requirements are clearly related to the adoption of dry seeding, which limits water applications to the field in the early months of the irrigation season. When looking at June, however, the water consumption in DFL (+25%) exceeds that required by FTI and DFLearly (about +5%), WFL (4.9 Mm³) and AWD (–28%). This happens because with dry seeding, paddy fields are flooded later in the season, and their filling, occurring when the groundwater level is low and the soil is dry, requires a huge volume of water. Among the dry seeded scenarios, FTI and DFLearly limit this occurrence: the first strategy because of the turned application of irrigation water, which lowers the volumes applied, and the second due to an earlier flooding of the paddies (about 10 days earlier). The AWD lower irrigation demand is linked to the adoption of wet seeding (shallower groundwater depth) but also to the start of the Alternate Wetting and Drying scheduling at the rice tillering phase (around the end of May).

The monthly Q_s are reported in Figure 10. DFL peak demand always surpasses the other simulated scenarios, overtaking them when the critical month of June or the late spring-early summer months are particularly dry. This is the case of the 2019 data, which is characterised by an extremely dry June, while in 2020 the presence of higher rainfall narrows the differences in total demand of the district between DFL and the other scenarios.

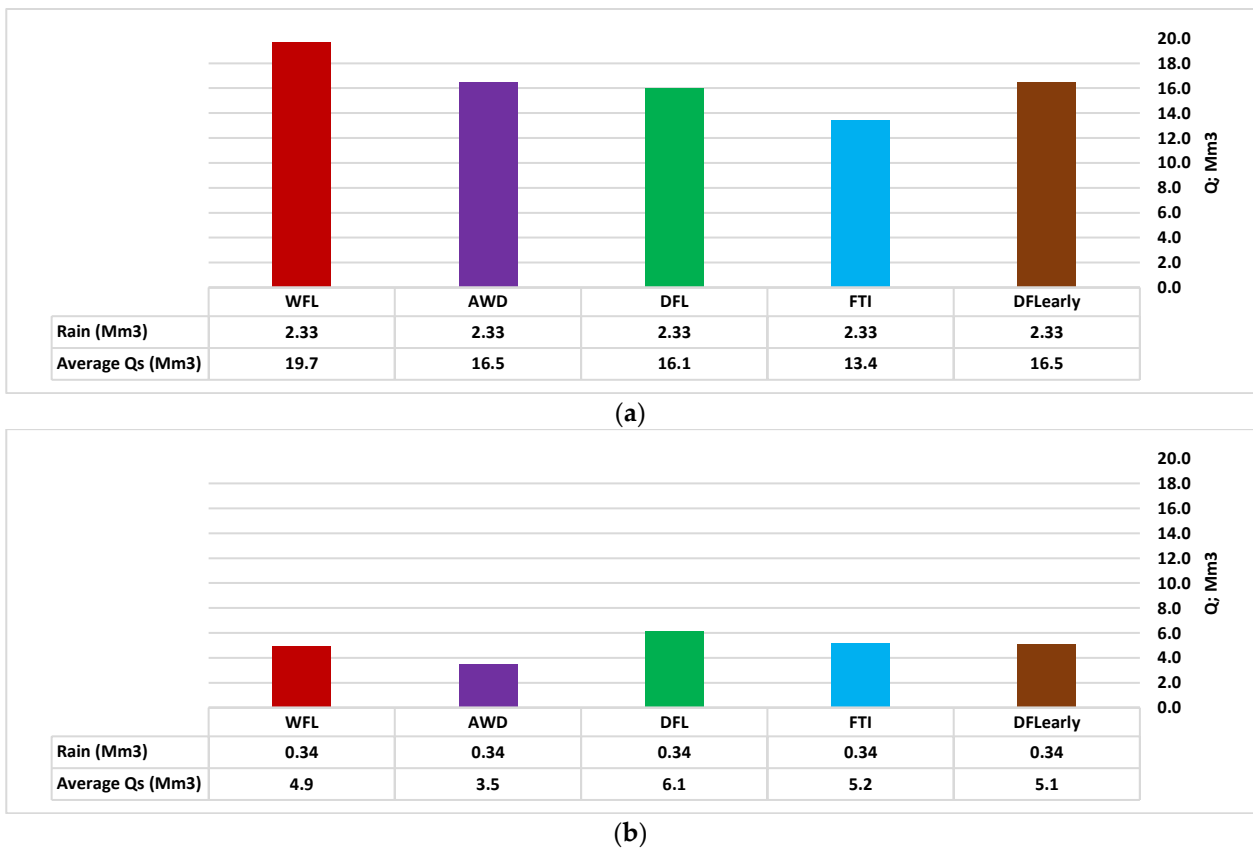


Figure 9. (a) Average seasonal (April–September) district total requirements (Q_s) simulated for the years 2013–2020; (b) Critical (June) district total requirements (Q_s) simulated for the years 2013–2020.

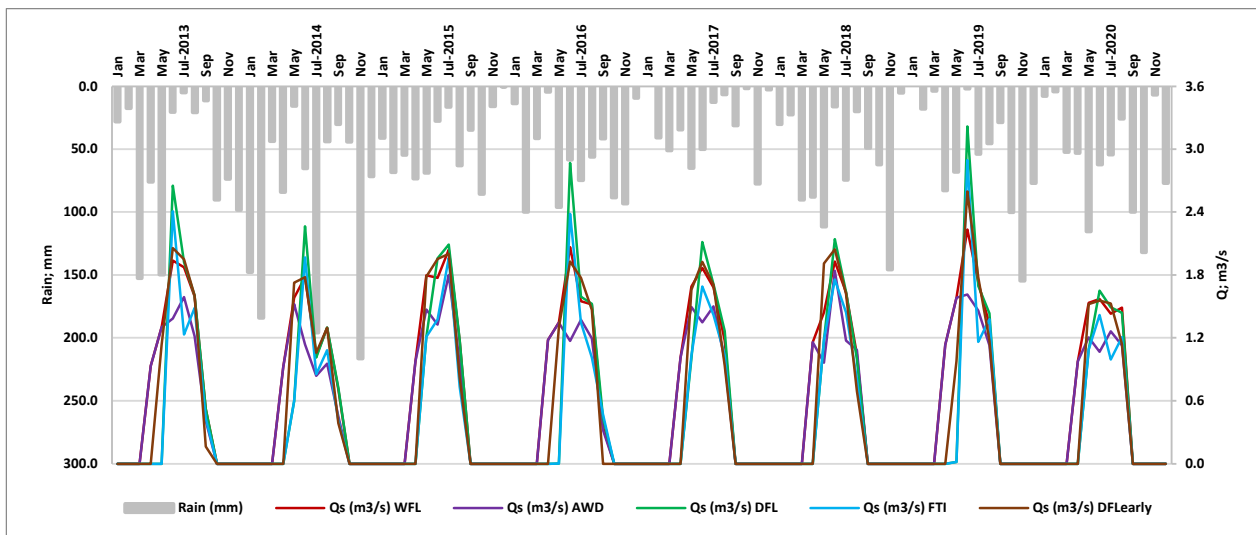
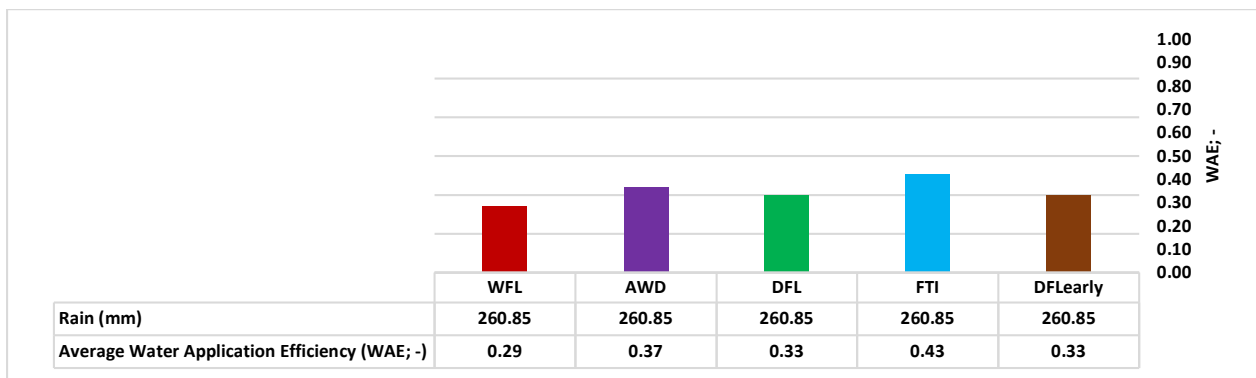


Figure 10. Monthly district total requirements (Q_s) simulated for the years 2013–2020.

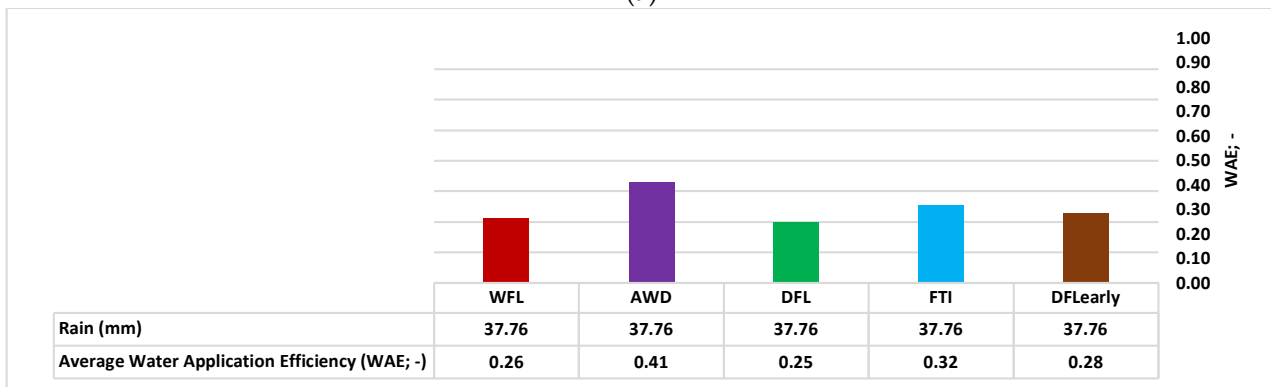
3.4. Water Application Efficiency

The seasonal average and critical Water Application Efficiency (WAE) are shown in Figure 11. During the season, FTI obtains the best WAE (0.43), followed by AWD (0.37), DFL and DFLeary (about 0.33) and WFL (0.29), which remains rather distant. On the other hand, when looking at the average WAE values for June, AWD (0.41) far exceeds FTI (0.32), DFLeary (0.28), WFL (0.26) and DFL (0.25). The AWD is the only scenario in which WAE

values remain relatively stable in both periods, showing a more efficient use of irrigation water at field level. FTI also shows good WAE values, but the fixed irrigation rotation scheme adopted in this technique seems to perform less well in the critical months of the irrigation season than the scheduling adopted in AWD, which is more linked to the actual rice water requirements. The good seasonal performance of the other dry seeding scenarios (DFL and DFLearly) seems to be more related to the adoption of dry seeding, which limits water consumption than to a real efficient use of water, given the very low WAE value in June. However, DFLearly seems to benefit from early seeding, showing slightly higher efficiency than DFL in June. As far as the efficiency of water use at field level is concerned, from the results presented, WFL is the least reliable scenario among those simulated.



(a)



(b)

Figure 11. (a) Average seasonal (April–September) Water Application Efficiency (WAE) calculated for the years 2013–2020; (b) Critical (June) Water Application Efficiency (WAE) calculated for the years 2013–2020.

3.5. Distribution Efficiency

Figure 12 displays the seasonal average and the critical Distribution Efficiency of the irrigation network (DE). DFL, WFL and DFLearly show a rather high seasonal DE (around 0.80), while AWD and FTI remain lower (around 0.70). During the whole season, continuous flooding techniques are clearly advantaged, as the shallower groundwater table limits the percolation from the channel network. In June, the flooding technique performs better, especially WFL (0.78) and DFLearly (0.72), but the dry seeding adopted in DFL (0.68) penalises this scenario in the most critical month. On the contrary, DFLearly continues to benefit from the early rise of the groundwater table due to early seeding. Deep groundwater depth conditions strongly influenced FTI (0.68) and AWD (0.66) efficiencies in June. In terms of channel efficiency, these latter two scenarios are the least performing of those simulated in both the aggregation periods.

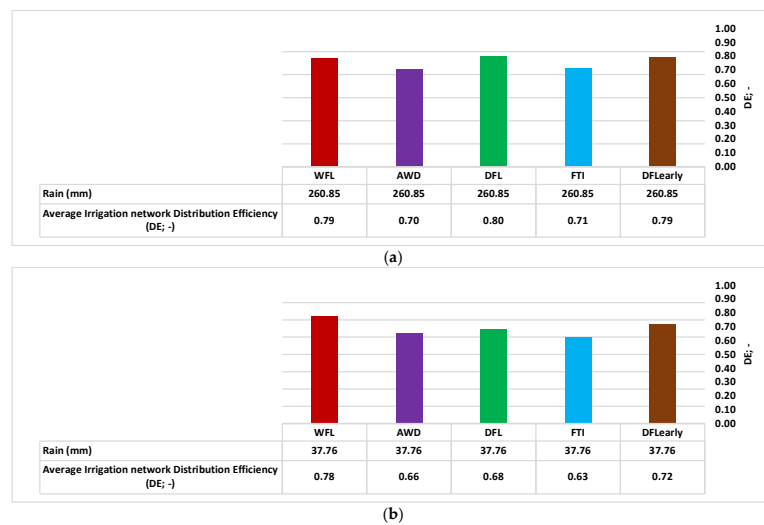


Figure 12. (a) Average seasonal (April–September) Distribution Efficiency (DE) calculated for the years 2013–2020; (b) Critical (June) Distribution Efficiency (DE) calculated for the years 2013–2020.

3.6. Relative Water Supply

Relative Water Supply (RWS) values are more connected to the overall efficiency of the irrigation strategies applied in the territory, since they consider both the irrigation efficiency of the agricultural land and the irrigation water losses in the channel system (Equation (9)). The seasonal and critical average RWS values are shown in Figure 13. In the simulated period, FTI (3.13) achieves the best seasonal RWS, closely followed by DFL (3.64) and AWD and DFLearly (about 3.70), showing a more efficient irrigation water use at the district level compared to WFL (4.33). However, in June, DFL (6.02) and FTI (5.13) show the worst RWS, while AWD (3.57) performs the best, followed by DFLearly (4.85) and WFL (4.89). Despite good seasonal values, the scenarios adopting dry seeding (DFL and FTI) are again adversely affected by the deeper groundwater depth conditions they experience in the early part of the season and close to the critical month of June, and thus by greater channel percolation that causes higher irrigation requirements, with a small exception for DFLearly due to the early seeding adopted. On the contrary, shallower groundwater levels in the case of WFL decrease channel percolation and raise the overall district water use efficiency. AWD seems to be the most robust scenario, with good performance both seasonally and in the critical month.

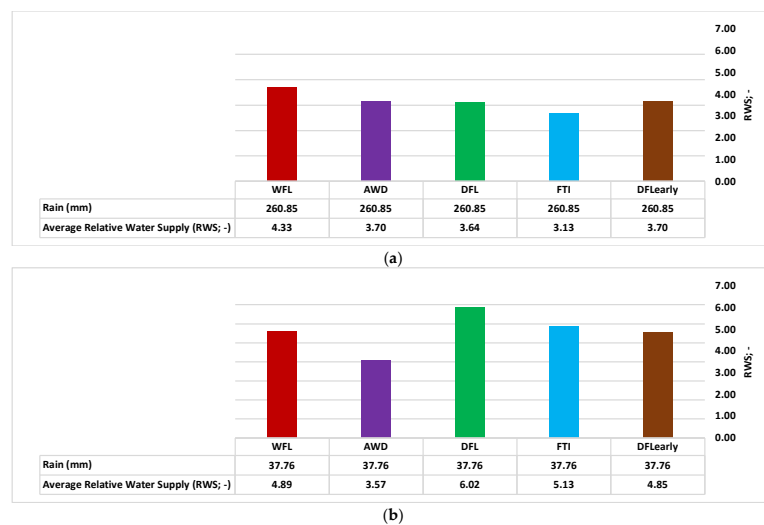


Figure 13. (a) Average seasonal (April–September) Relative Water Supply (RWS) calculated for the years 2013–2020; (b) Critical (June) Relative Water Supply (RWS) calculated for the years 2013–2020.

4. Conclusions

The modeling work conducted in this study once again highlighted the strong connection between irrigation management and groundwater table in rice-growing areas characterised by shallow aquifers, which makes it complex to estimate the actual efficiency of irrigation management alternatives over vast agricultural areas without the implementation of articulated agro-hydrological tools such as the one proposed in the paper.

Recently, many portions of the rice-growing area in the Padana Plain are facing a lowering of the groundwater table at the beginning of the agricultural season due to a massive conversion to dry-seeded irrigation techniques. However, even if this strategy is able to reduce the total irrigation volume used during the irrigation season (April–September), as demonstrated for the dry seeding and delayed flooding (DFL) scenario in this study, it does not allow to decrease the irrigation demand in the most critical month of the season (June/July), leading to an even higher irrigation demand when compared with the wet seeding and continuous flooding (WFL), and the wet seeding and Alternate Wetting and Drying (AWD). The calculated Relative Water Supply (RWS) values for the DFL clearly show a less efficient district water use compared to the other scenarios simulated.

Early seeding DFL (DFLearly) can benefit from an anticipated seeding date than its original formulation, showing a better RWS than DFL in the critical month of the season, which is comparable to that of WFL but still far from the one achieved with AWD. However, rice varieties different from those used at the present time should be identified to meet appropriate thermal conditions for germination and/or to avoid yield and product quality losses if the grain-filling period falls during high temperature periods.

Although dry seeding and fixed-turn irrigation (FTI) performs better than DFL and DFLearly throughout the irrigation season, mainly due to a reduction of irrigation volumes applied at the field level, in June/July the dry seeding technique adopted and the rigid irrigation scheme employed severely penalise its performance in terms of water use and, consequently, in the calculated RWS index.

A safe AWD, applied after a wet seeding, seems to be a suitable solution to reduce irrigation demand for rice after the tillering phase (late May–early June) while maintaining good groundwater recharge, especially in the early part of the season (until the end of May). AWD achieves good performances on a seasonal basis—in particular in June/July—when it records by far the highest RWS value. AWD simulated water savings compared to WFL (16%) are less than those found at the field level at CRR-ENR (25% in 2021–2022 and 20% in 2019–2020; see Section 2.4 Simulated scenarios) and reported in the meta-analysis [7] (23.4%), which are indeed in a good agreement with each other. The coarser texture and the overall deeper water table condition (see Figures 6 and 8) in the San Giorgio di Lomellina pilot district are likely responsible for the lower water savings compared to those measured at CRR-ENR. In addition, it is important to highlight that the considered studies refer to results obtained in field trials, which do not consider water distribution network losses. In any case, based on the results obtained, we can state that, if implemented over large agricultural areas, AWD could be a good option to cope with low groundwater levels at the beginning of the season and to appease the exasperated competition for water among crops that the rice-growing area of northern Italy has been experiencing in recent years.

A massive change in irrigation management introduced by decision makers to target one or more environmental benefits may be considered if it is also economically beneficial to farmers. In a further work, data collected in [36] and the results presented here will be used to broaden the assessment of the AWD sustainability in rice-systems of northern Italy using appropriate economic, environmental and social acceptability indicators [37]. From the hydrological point of view, in order to better support decision making, the modelling framework presented in this study will be applied to reproduce the effect of rice irrigation management strategies on the water balance in rice areas on a regional basis. However, changes to some of the implemented approaches as a consequence of the simulation scale enlargement and of the actual data availability need to be discussed.

Author Contributions: Conceptualization, M.R. (Michele Rienzner) and A.F.; Data curation, G.L.C.G., A.M. and M.R. (Michele Rienzner); Formal analysis, G.L.C.G., A.M., M.R. (Michele Rienzner) and A.F.; Funding acquisition, M.R. (Marco Romani) and A.F.; Methodology, G.L.C.G., A.M., M.R. (Michele Rienzner), M.R. (Marco Romani) and A.F.; Project administration, A.F.; Software, G.L.C.G., A.M. and M.R. (Michele Rienzner); Supervision, A.F.; Validation, G.L.C.G., A.M., M.R. (Michele Rienzner), M.R. (Marco Romani) and A.F.; Visualization, G.L.C.G.; Writing—original draft, G.L.C.G. and A.F.; Writing—review and editing, G.L.C.G., M.R. (Michele Rienzner), M.R. (Marco Romani) and A.F. All authors have read and agreed to the published version of the manuscript.

Funding: Publication carried out under the following two research projects: (1) no. 6 RISWAGEST ‘Gestione innovativa dell’acqua in risaia’ selected under the Lombardy Region’s Call for Research Projects in Agriculture and Forestry 2018 (d.d.s. 5 March 2020—No. 2955); (2) The international MED-WATERICE project ‘Towards a sustainable water use in Mediterranean rice-based agro-ecosystems’ (<https://www.medwaterice.org/>), selected in 2018 in the context of the PRIMA Program (<https://prima-med.org/>; PRIMA-Section2–2018) and funded, for the Italian partners, by the MUR (Italian Ministry of University and Research).

Data Availability Statement: The data presented in this study are available on request from the corresponding author.

Acknowledgments: We wish to thank the Associazione Irrigazione Est Sesia (AIES) for the data provided and the support given to this research.

Conflicts of Interest: The authors declare no conflict of interest.

Nomenclature

AIES	Associazione Irrigazione Est Sesia (Irrigation Consortia)
AWD	Alternate Wetting and Drying after a wet seeding
CP	Model used to estimate the monthly Percolation from the Channel network (one of the three sub-models of the modelling framework).
DE	Distribution Efficiency of the irrigation network (-).
DFL	Dry seeding and delayed FLOODing.
DFLearly	Early Dry seeding and delayed FLOODing.
DVS	Crop Development Stage (-).
ENR	Ente Nazionale Risi (the National Rice Authority in Italy).
FTI	Dry seeding and Fixed-Turn Irrigation.
GWD	GroundWater Depth below the soil surface (m).
GWL	GroundWater Level (m a.s.l.)
PGL	Model used to estimate the average monthly Groundwater Level from the Percolation (one of the three sub-models of the modelling framework).
RWS	Relative Water Supply (-).
SDMAA	Semi-Distributed Model for the Agricultural Area (one of the three sub-models of the modelling framework).
SWAP	Soil Water Atmosphere Plant model, core model for the SDMAA
WAE	Water Application Efficiency (-).
WFL	Wet seeding and continuous Flooding.

References

1. GRiSP (Global Rice Science Partnership). *Rice Almanac: Source Book for One of the Most Important Economic Activities on Earth*, 4th ed.; IRRI: Los Baños, Philippines, 2013; ISBN 978-971-22-0300-8.
2. Nayar, N.M. *Origins and Phylogeny of Rices*; Elsevier: Amsterdam, The Netherlands; Academic Press: Cambridge, MA, USA, 2014; ISBN 978-0-12-417177-0.
3. Chauhan, B.S.; Jabran, K.; Mahajan, G. *Rice Production Worldwide*; Springer International Publishing: Cham, Switzerland, 2017; ISBN 978-3-319-47514-1.
4. Gassman, P.W.; Jeong, J.; Boulange, J.; Narasimhan, B.; Kato, T.; Somura, H.; Watanabe, H.; Eguchi, S.; Cui, Y.; Sakaguchi, A.; et al. Simulation of rice paddy systems in SWAT: A review of previous applications and proposed SWAT + rice paddy module. *Int. J. Agric. Biol. Eng.* **2022**, *15*, 1–24. [[CrossRef](#)]
5. Liu, X.; Liu, W.; Tang, Q.; Liu, B.; Wada, Y.; Yang, H. Global Agricultural Water Scarcity Assessment Incorporating Blue and Green Water Availability Under Future Climate Change. *Earths Future* **2022**, *10*, e2021EF002567. [[CrossRef](#)]

6. Lampayan, R.M.; Rejesus, R.M.; Singleton, G.R.; Bouman, B.A. Adoption and economics of alternate wetting and drying water management for irrigated lowland rice. *Field Crops Res.* **2015**, *170*, 95–108. [CrossRef]
7. Carrijo, D.R.; Lundy, M.E.; Linquist, B.A. Rice yields and water use under alternate wetting and drying irrigation: A meta-analysis. *Field Crops Res.* **2017**, *203*, 173–180. [CrossRef]
8. Linquist, B.A.; Anders, M.M.; Adviento-Borbe, M.A.A.; Chaney, R.L.; Nalley, L.L.; Da Rosa, E.F.F.; van Kessel, C. Reducing greenhouse gas emissions, water use, and grain arsenic levels in rice systems. *Glob. Chang. Biol.* **2015**, *21*, 407–417. [CrossRef]
9. Liang, K.; Zhong, X.; Huang, N.; Lampayan, R.M.; Pan, J.; Tian, K.; Liu, Y. Grain yield, water productivity and CH₄ emission of irrigated rice in response to water management in south China. *Agric. Water Manag.* **2016**, *163*, 319–331. [CrossRef]
10. Tuong, P.; Bouman, B.; Mortimer, M. More Rice, Less Water—Integrated Approaches for Increasing Water Productivity in Irrigated Rice-Based Systems in Asia. *Plant Prod. Sci.* **2005**, *8*, 231–241. [CrossRef]
11. Kroes, J.; van Dam, J.; Supit, I.; de Abelleira, D.; Verón, S.; de Wit, A.; Boogaard, H.; Angelini, M.; Damiano, F.; Groenendijk, P.; et al. Agrohydrological analysis of groundwater recharge and land use changes in the Pampas of Argentina. *Agric. Water Manag.* **2019**, *213*, 843–857. [CrossRef]
12. Li, P.; Ren, L. Evaluating the effects of limited irrigation on crop water productivity and reducing deep groundwater exploitation in the North China Plain using an agro-hydrological model: I. Parameter sensitivity analysis, calibration and model validation. *J. Hydrol.* **2019**, *574*, 497–516. [CrossRef]
13. Li, P.; Ren, L. Evaluating the effects of limited irrigation on crop water productivity and reducing deep groundwater exploitation in the North China Plain using an agro-hydrological model: II. Scenario simulation and analysis. *J. Hydrol.* **2019**, *574*, 715–732. [CrossRef]
14. Siad, S.M.; Iacobellis, V.; Zdruli, P.; Gioia, A.; Stavi, I.; Hoogenboom, G. A review of coupled hydrologic and crop growth models. *Agric. Water Manag.* **2019**, *224*, 105746. [CrossRef]
15. Uniyal, B.; Dietrich, J. Simulation of Irrigation Demand and Control in Catchments—A Review of Methods and Case Studies. *Water Resour. Res.* **2021**, *57*, e2020WR029263. [CrossRef]
16. Singh, R.; Kroes, J.G.; van Dam, J.C.; Feddes, R.A. Distributed ecohydrological modelling to evaluate the performance of irrigation system in Sirsa district, India: I. Current water management and its productivity. *J. Hydrol.* **2006**, *329*, 692–713. [CrossRef]
17. Singh, R.; Jhorar, R.K.; van Dam, J.C.; Feddes, R.A. Distributed ecohydrological modelling to evaluate irrigation system performance in Sirsa district, India II: Impact of viable water management scenarios. *J. Hydrol.* **2006**, *329*, 714–723. [CrossRef]
18. Li, Y.; Šimůnek, J.; Jing, L.; Zhang, Z.; Ni, L. Evaluation of water movement and water losses in a direct-seeded-rice field experiment using Hydrus-1D. *Agric. Water Manag.* **2014**, *142*, 38–46. [CrossRef]
19. Gulati, D.; Satpute, S.; Kaur, S.; Aggarwal, R. Estimation of potential recharge through direct seeded and transplanted rice fields in semi-arid regions of Punjab using HYDRUS-1D. *Paddy Water Environ.* **2022**, *20*, 79–92. [CrossRef]
20. Richards, L.A. Capillary Conduction of Liquids through Porous Mediums. *Physics* **1931**, *1*, 318–333. [CrossRef]
21. Tsuchiya, R.; Kato, T.; Jeong, J.; Arnold, J. Development of SWAT-Paddy for Simulating Lowland Paddy Fields. *Sustainability* **2018**, *10*, 3246. [CrossRef]
22. Kamruzzaman, M.; Hwang, S.; Choi, S.-K.; Cho, J.; Song, I.; Song, J.; Jeong, H.; Jang, T.; Yoo, S.-H. Evaluating the Impact of Climate Change on Paddy Water Balance Using APEX-Paddy Model. *Water* **2020**, *12*, 852. [CrossRef]
23. Kim, D.-H.; Jang, T.; Hwang, S. Evaluating impacts of climate change on hydrology and total nitrogen loads using coupled APEX-paddy and SWAT models. *Paddy Water Environ.* **2020**, *18*, 515–529. [CrossRef]
24. FAOSTAT. Available online: <https://www.fao.org/faostat/en/#home> (accessed on 5 April 2023).
25. Monaco, S.; Volante, A.; Orasen, G.; Cochrane, N.; Oliver, V.; Price, A.H.; Teh, Y.A.; Martínez-Eixarch, M.; Thomas, C.; Courtois, B.; et al. Effects of the application of a moderate alternate wetting and drying technique on the performance of different European varieties in Northern Italy rice system. *Field Crops Res.* **2021**, *270*, 108220. [CrossRef]
26. Kroes, J.G.; van Dam, J.C.; Bartholomeus, R.P.; Groenendijk, P.; Heinen, M.; Hendriks, R.F.A.; Mulder, H.M.; Supit, I.; van Walsum, P.E.V. *SWAP Version 4, Wageningen Environmental Research Report*; No. 2780; Wageningen Environmental Research: Wageningen, The Netherlands, 2017.
27. Mayer, A.; Rienzner, M.; Cesari de Maria, S.; Romani, M.; Lasagna, A.; Facchi, A. A Comprehensive Modelling Approach to Assess Water Use Efficiencies of Different Irrigation Management Options in Rice Irrigation Districts of Northern Italy. *Water* **2019**, *11*, 1833. [CrossRef]
28. Ente Nazionale Risi-ENR. Available online: https://www.enterisi.it/servizi/notizie/notizie_homepage.aspx (accessed on 5 April 2023).
29. Agenzia Regionale per la Protezione dell’Ambiente-ARPA Lombardia. Available online: https://www.arpalombardia.it/Pages/ARPA_Home_Page.aspx (accessed on 6 April 2023).
30. Associazione Irrigazione Est Sesia-AIES. Available online: <https://www.estsesia.it/> (accessed on 6 April 2023).
31. Geoportale Lombardia. Available online: <https://www.geoportale.regione.lombardia.it/> (accessed on 6 April 2023).
32. Tomasella, J.; Hodnett, M.G. Estimating soil water retention characteristics from limited data in brazilian amazonia. *Soil Sci.* **1998**, *163*, 190–202. [CrossRef]
33. Ungaro, F.; Calzolari, C.; Busoni, E. Development of pedotransfer functions using a group method of data handling for the soil of the Pianura Padano-Veneta region of North Italy: Water retention properties. *Geoderma* **2005**, *124*, 293–317. [CrossRef]
34. Xu, H. Modification of normalised difference water index (NDWI) to enhance open water features in remotely sensed imagery. *Int. J. Remote Sens.* **2006**, *27*, 3025–3033. [CrossRef]

35. Moriasi, D.N.; Arnold, J.G.; van Liew, M.W.; Bingner, R.L.; Harmel, R.D.; Veith, T.L. Model Evaluation Guidelines for Systematic Quantification of Accuracy in Watershed Simulations. *Trans. ASABE* **2007**, *50*, 885–900. [[CrossRef](#)]
36. Facchi, A.; Gharsallah, O.; Romani, M.; Arbat, G.; Cufí, S.; Ramírez de Cartagena, F.; Pinsach, J.; Mira, C.; Mateos, L.; de Lima, I.P.; et al. Irrigation strategies alternative to continuous flooding to decrease water use and increase water productivity in Mediterranean rice-based agroecosystems. In Proceedings of the Interregional Conference Sustainable Production in Agroecosystems with Water Scarcity (SUPWAS), Albacete, Spain, 5–7 September 2022.
37. Gharsallah, O.; Facchi, A.; Gilardi, G.; Corsi, S.; Vuciterna, R.; Romani, M.; Cadei, E.; Trevisan, M.; Lamastra, L.; Voccia, D.; et al. Economic, environmental, and social sustainability of water-saving solutions for the rice sector in the Mediterranean basin. In Proceedings of the Interregional Conference Sustainable Production in Agroecosystems with Water Scarcity (SUPWAS), Albacete, Spain, 5–7 September 2022.
38. Bouman, B.; Peng, S.; Castañeda, A.R.; Visperas, R.M. Yield and water use of irrigated tropical aerobic rice systems. *Agric. Water Manag.* **2005**, *74*, 87–105. [[CrossRef](#)]
39. Bos, M.G.; Burton, M.A.S.; Molden, D.J. *Irrigation and Drainage Performance Assessment: Practical Guidelines*; CABI Pub: Wallingford Oxfordshire, UK; Cambridge, MA, USA, 2005; ISBN 0851999670.

Disclaimer/Publisher’s Note: The statements, opinions and data contained in all publications are solely those of the individual author(s) and contributor(s) and not of MDPI and/or the editor(s). MDPI and/or the editor(s) disclaim responsibility for any injury to people or property resulting from any ideas, methods, instructions or products referred to in the content.